ARCHIVES
of
FOUNDRY ENGINEERING

ISSN (2299-2944)
Volume 2025
Issue 3/2025

94 – 104

11/3

10.24425/afe.2025.155358

Published quarterly as the organ of the Foundry Commission of the Polish Academy of Sciences

Characteristics of Retained Austenite in Cast GX70CrMnSiNiMo2 Alloy Tool Steel

G. Tęcza *, A. Garbacz-Klempka
AGH University of Krakow, Poland
* Corresponding author: E-mail address: tecza@agh.edu.pl

Received 17.01.2025; accepted in revised form 12.03.2025; available online 23.07.2025

Abstract

Material wear strictly depends on hardness and microstructure, homogeneity of this microstructure in particular. The presence of retained austenite in the microstructure is not always the cause of the reduced wear resistance, though it is commonly believed that retained austenite has low hardness and is responsible for the accelerated wear of components. The aim of this study is to demonstrate that the hardness of retained austenite is similar to that of martensite and can even reach 900HV0.2, while its volume fraction, which for the tested alloy amounts to about 21%, depends to a very small extent only on the cooling intensity of the quenching medium. Reducing the cooling rate by quenching in air, when the cooling rate is the lowest, makes the volume fraction V_v of retained austenite increase to even 31%, while its hardness assumes the lowest value and decreases to slightly over 800HV0.2, similarly to the hardness of martensite, which decreases on average to approximately 850HV0.2. The occurrence of retained austenite and its high hardness should be associated with the primary segregation of elements such as Cr, Mo, Mn, Si, whose content assumes the highest values in the interdendritic areas.

Keywords: Retained austenite, Martensite, Microstructure, Microhardness, Phase volume fraction, Heat treatment, Quenching, Cast tool steel

1. Introduction

It is commonly believed that retained austenite is characterized by low hardness and is a harmful structural constituent in castings, mainly because its volume increases during transformation into martensite, which causes the formation of structural stresses and even cracks. Its presence can result in the dimensional instability of components over time (e.g. components after grinding) and reduces both hardness and strength of parts as well as the corrosion resistance. Yet, besides its unfavourable effects, there are also some positive aspects of the presence of retained austenite, i.e. the reduced tendency of castings to brittle fracture, combined with higher fatigue strength and abrasion resistance [1-7]. Presented in this way, the characteristics of retained austenite seem to be very inconsistent, and therefore an attempt has been made to study the chemical composition and changes in hardness in the two examined areas of martensite and retained austenite in cast GX70CrMnSiNiMo2 tool steel.

Retained austenite is the austenite that did not undergo transformation into martensite during martensitic transformation and after its completion. The reason why the martensitic transformation is incomplete is, firstly, the larger volume of martensite compared to austenite (~4% at 1wt.% C, sometimes even up to 6%) – the austenite is "compressed" and, secondly, can not reach the end temperature of the transformation, which decreases with the increasing content of carbon and alloying elements [1]. Figure 1 shows a relationship between the content of retained austenite and carbon content in unalloyed steel. Figure 2 shows the effect of carbon on the position of the *Ms* temperature and *Mf* temperature for unalloyed steels, remembering that the addition of alloying elements such as Mn, Cr, Mo, Ni, Si only further reduces these values (Fig. 3) [1].

© The Author(s) 2025. Open Access. This article is licensed under a Creative Commons Attribution 4.0 International License (http://creativecommons.org/licenses/by/4.0/), which permits use, sharing, adaptation, distribution and reproduction in any medium or format, as long as you give appropriate credit to the original author(s) and the source, provide a link to the Creative Commons licence, and indicate if changes were made.

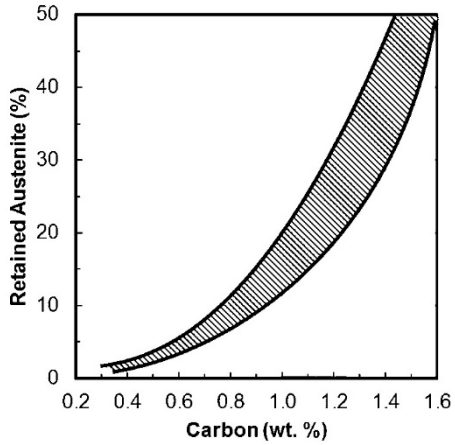

Fig. 1. Retained austenite as a function of carbon content for plain carbon steels quenched to room temperature [8]

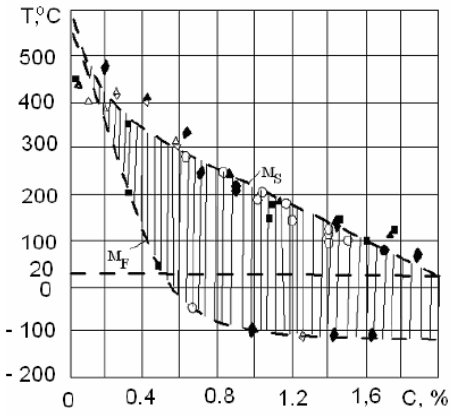

Fig. 2. Martensite start temperature (*Ms*) and martensite finish temperature (*Mf*) versus carbon content in steel [9]

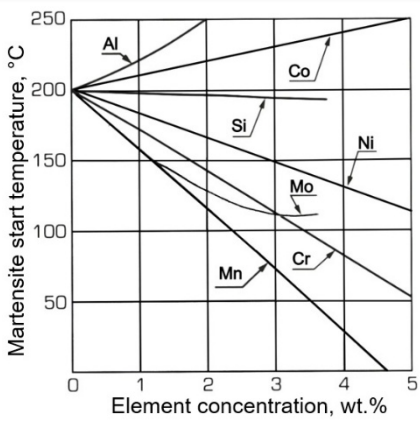

Fig. 3. Effect of Cr, Mn, Si, Ni and Mo on the value of the *Ms* temperature [3]

As follows from Figures 1 and 2, in steel with a carbon content of 0.7 wt.%, the presence of retained austenite should always be expected, and among other factors that affect its amount and result from the process of heat treatment, one should mention the higher temperature of austenitizing, which increases the tendency of austenite to transform, and the degree of the steel undercooling below the *Ms* temperature; with a low rate of undercooling, more austenite is transformed into martensite [1].

Therefore, when quenching alloys with a high carbon content and with the addition of elements that increase hardenability, it is always necessary to consider the advisability of carrying out the heat treatment based on freezing, which is one of the methods of reducing the amount of retained austenite in steel after quenching.

The cast GX70CrMnSiNiMo2 alloy tool steel, which contains on average 0.7 wt.% C, 1.0 wt.% Mn, 0.5 wt.% Si, 1.8 wt.% Cr, 0.6 wt.% Ni and 0.4 wt.% Mo, is used primarily for cast machine and device components operating in the sectors of industry such as mining, quarrying, aggregate processing, materials processing and energy. These are branches of heavy industry where alloys resistant to abrasive wear are used, mainly as large-sized thick-walled castings of coal grinding sets in coal-fired power plants.

The chemical composition of this cast steel is selected in such a way as to enable quenching of castings in air. On the other hand, owing to an appropriately selected tempering temperature, it is possible to control the hardness and plasticity of the manufactured parts. Figure 3 shows examples of the characteristic microstructures of cast GX70CrMnSiNiMo2 steel. The as-cast steel usually has a pearlitic structure (Fig. 4a), which after quenching becomes purely martensitic (Fig. 4b). Sometimes, however, the increased content of carbon and numerous alloying elements (Mn, Cr, Si, Ni and Mo) hinder obtaining a homogeneous martensitic microstructure during hardening, and a certain amount of retained austenite is left in the microstructure (Fig. 4c) [10]. This type of microstructure can cause uneven hardness on the casting surface and contribute to uneven and accelerated wear of machine parts during operation, especially when these are balls and raceways of coal mills.

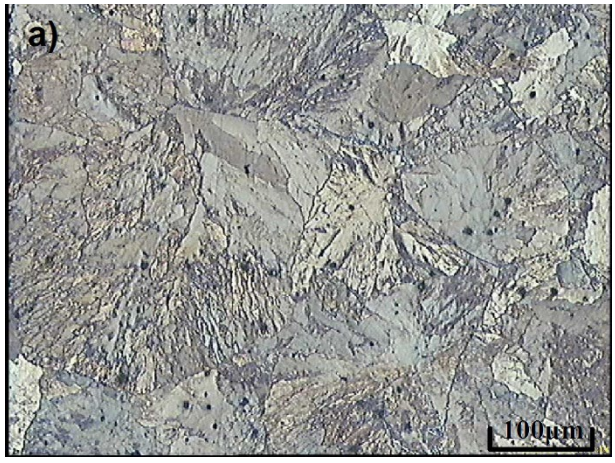

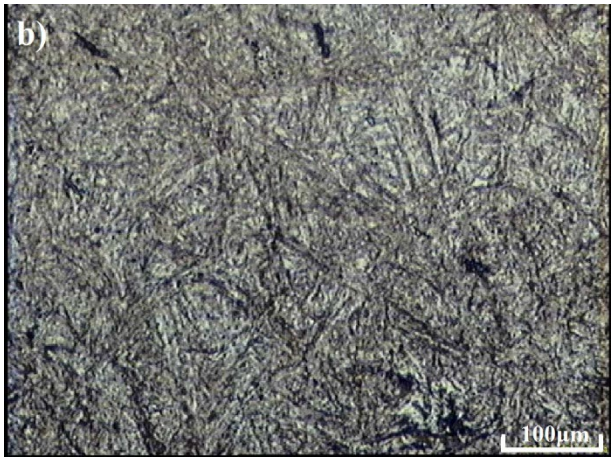

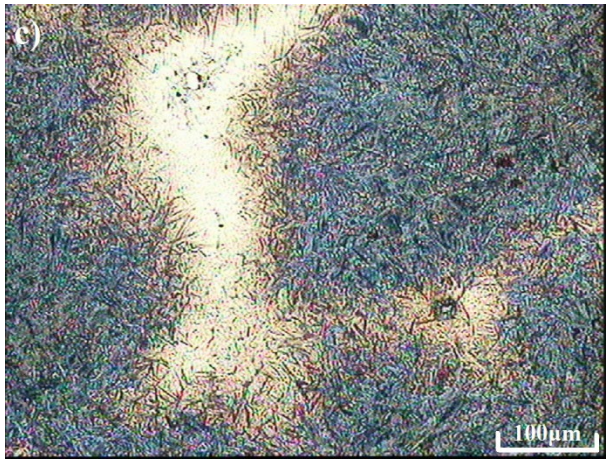

Fig. 4. Microstructure of cast GX70CrMnSiNiMo2 steel: a) as-cast, pearlite; b) after quenching, martensite; c) after quenching, dark martensite, light retained austenite; etched with nital [10]

Even in earlier studies, the Author and his colleagues made some interesting observations. They reported that in the cast GX70CrMnNiMo2 steel (without Si) after heat treatment, which consisted in quenching from 960°C and tempering at 450°C, a maximum of about 4% of retained austenite was observed, the hardness of which measured by the Vickers method under a load of 20 g ranged between 600 and 750 HV0.02. Unfortunately, hardness values in the martensitic areas are not provided in this study, but based on the available microstructures examined at the same magnification, it is easy to note that the size of the indentations left by microhardness measurements is larger in the martensitic areas, which indicates a lower hardness of that constituent. Figure 5 presents and compares the images of the areas of martensite and retained austenite with visible indentations. Figure 5b also clearly shows that individual hardness measurements were made within single austenite grains [11].

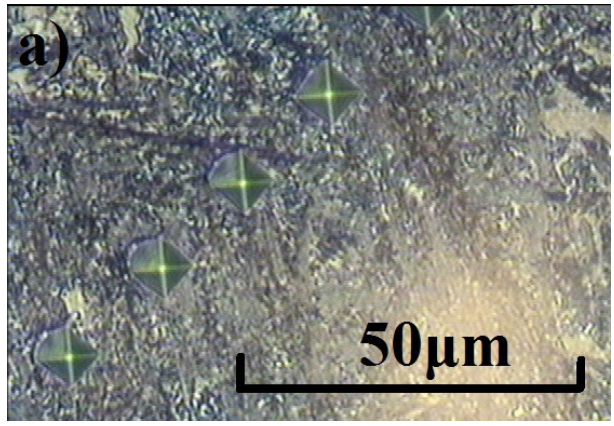

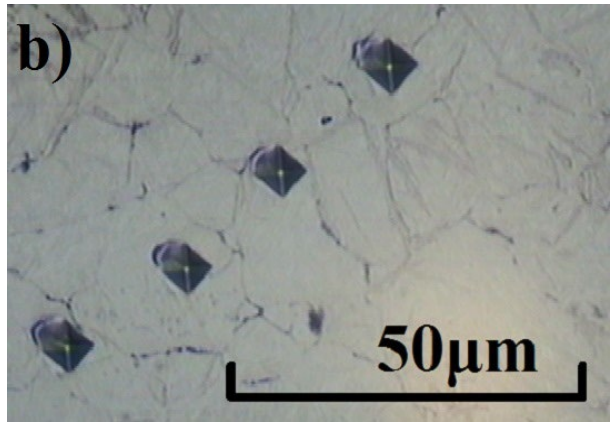

Fig. 5. Microstructure of cast GX70CrMnNiMo2 steel with visible imprints left by hardness measurements: a) in the area of martensite, b) in the area of retained austenite [11]

This situation may indeed occur in practice, because the areas of austenite are compressed from all sides by martensite and additional primary segregation of alloying elements into the interdendritic spaces further increases hardness obtained by solid solution hardening.

Interesting studies found in the literature include [8,12], where the authors only indicate and outline possible methods of determining the amount of retained austenite in steel, comparing light microscopy that provides qualitative assessment, magnet inductive measurements that must be calibrated to specific materials, EBSD measurements, the results of which are somewhat similar to XRD, and XRD measurements, which work for homogeneous steels. In [13], the mechanical stability of retained austenite and its transformation into martensite in high-carbon and low-carbon steels was studied. In [14], the effect of silicon and manganese content on the volume fraction and stability of retained austenite in dual-phase TRIP steels was presented. In [15], the research focused on silicon-manganese steels with carbon content of 0.25, 0.33 and 0.44 wt.% and with a variable content of retained austenite, which improved uniform elongation, resulting in an excellent combination of strength and plasticity. The authors of [16] examined the effect of austenitization temperature from 1000 to 1150°C for 10-60 min. on the decrease in hardness with

increasing volume fraction of retained austenite, but the material examined was steel and not cast steel.

Studies of retained austenite rarely include the effect of heat treatment parameters on its volume fraction or hardness; they mainly concern steel and the presence of retained austenite is only mentioned. Among the research works on cast steel, particular attention deserves [17], where attention is focused on the volume fraction of retained austenite and carbon content in this austenite in cast high-silicon steel after tempering at different temperatures (240-400°C). Experiments have shown that both volume fraction of retained austenite and carbon content in this austenite are low at low tempering temperatures, and with the increase in tempering temperature, both volume fraction of retained austenite and carbon content in this austenite gradually increase. The most interesting seems to be the research described in [18], where the combined effect of liquid steel modification and heat treatment on the obtained microstructure and properties of cast Mn–Si–Cr steel has been taken into consideration. It has been shown that after modification with magnesium and rare earth metals, a uniform hardness was obtained, the microstructure became more homogeneous and the grains were refined. Additionally, after the applied heat treatment, the amount of retained austenite decreased and the amount of carbides increased. Impact strength increased by 20% and wear resistance was by 38% higher than the wear resistance of the unmodified sample.

2. Test materials and methods

Test samples were cut out from the external surface of the casting in a lower part of the main metal feeding system. The casting was a ball intended for operation in a coal mill. It had a circular cross-section and a wall thickness of 80 mm. The respective diagram is shown in Figure 6. Only sections from the outside of the cylinder with dimensions of about 20x20x20 mm were selected for the tests to ensure that the possible porosity formed during solidification in the circular cross-sections of the cylinder had no effect on the obtained results. The tested samples are marked in blue in Figure 6.

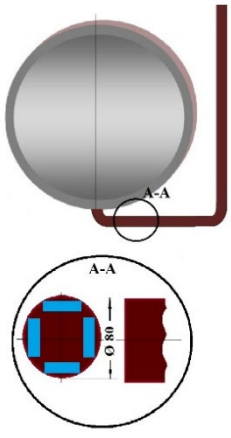

Fig. 6. Diagram of the system feeding metal to the casting of ball and places where the test samples were cut out marked in blue

The analysis of the chemical composition was performed under industrial conditions with a Foundry Master Smart spark spectrometer and repeated under laboratory conditions using a Spectro Maxx LMF04 spectrometer. Table 1 compares the average chemical composition from both analyses of the tested cast steel.

Based on the analysis of the chemical composition of the tested samples, it was found that the tested cast steel contained on average 0.72 wt.% of carbon, which should provide sufficient hardness of martensite after quenching, and additionally 0.46 wt.% Si, 1.02 wt.% Mn, 1.94 wt.% Cr, 0.66 wt.% Ni and 0.47 wt.% Mo, which should confer sufficient hardenability to the tested alloy. The content of V and Nb at the level of 0.017 and 0.014 wt.%, respectively, does not indicate deliberate modification of the liquid steel in the ladle, while the content of Al increased to 0.06 wt.% indicates correct, probably two-stage deoxidation of the steel in the ladle before casting. The content of P and S impurities at the level of 0.045 and 0.018 wt.%, respectively, has no major effect on the hardenability of the tested alloys and their hardness after quenching.

Examinations of microstructure were carried out on the prepared metallographic sections using a Kern Optics light microscope and a Leica MEF 4M light microscope; both devices are equipped with a camera and a system for automatic, digital image recording.

The as-cast microstructure of the tested cast steel consists of pearlite with hardness from 224 to 311 HV0.2 (an average of 275 HV0.2 from thirteen measurements). Figure 7 shows an example of a pearlitic microstructure of the tested cast steel with visible imprints left by the microhardness measurements. The size of the imprints corresponds to an average hardness of 275 HV0.2.

Microhardness tests were performed by the Vickers method using a Prazision HV1000B hardness tester under a load of 200 g for both as-cast and heat-treated samples. The average hardness of martensite and retained austenite was calculated from at least ten measurements.

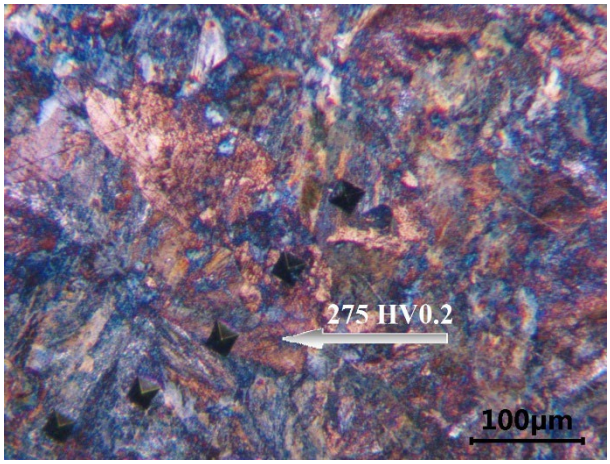

Fig. 7. Example of as-cast microstructure of the examined steel, pearlite; etched with nital

Table 1.
Chemical composition of the tested cast steel

Chemical Composition [wt.%]											
C	Si	Mn	P	S	Cr	Ni	Mo	V	Nb	B	Al
0.72	0.46	1.02	0.045	0.018	1.94	0.66	0.47	0.017	0.014	0.002	0.06

The prepared samples with a wall thickness of 20 mm were heated for 0.7 h and quenched from a temperature of 930°C in different cooling media to enable determination of the effect of cooling rate on the volume fraction and hardness of martensite and retained austenite. The use of extremely different cooling media had an additional aim, namely to cause the formation of hardening cracks, the examination of which should indicate the areas through which the cracks were running, the areas where they originated, and the areas which were particularly sensitive to crack formation. Cooling in air and water was applied, as well as cooling at intermediate rates in a 10, 20, and 30% aqueous solution of Polihartenol HI polymer (for induction hardening). The choice of this type of polymer was due to the small dimensions of the samples (20 mm) and a relatively easy preparation of the solution, the cooling intensity of which depends on the concentration and decreases with increasing concentration. Immediately after quenching, all samples were annealed at a temperature of 200°C for one hour.

The phase composition of the tested samples was checked with a Siemens Kristalloflex 4H X-ray diffractometer, using characteristic Cu radiation (Kα = 0.154 nm) at a step of 0.05 2theta/1s.

On the obtained images of microstructure, using the grid method which is one of the variants of the point method, the volume fraction V_v of retained austenite was calculated as the quotient of the number of points incident on the phase of interest (*RA*) and the total number of points plotted on the microstructure (Eq. 1). The measurement was performed for a total number of points equal to 1404 (12 applications of a grid with dimensions of 13x9 points for a given heat treatment variant). The selected method and manual measurement eliminate the error that may result from classifying a given area of the macrostructure as martensite or retained austenite A_{sz}, which happens in the case of automatic measurements, when a given area is classified based on the colour shades obtained for the examined phases and, depending on the colour intensities obtained during etching of the tested samples, may be incorrectly classified.

$$V_V = P_P = \frac{\sum_{i=1}^{k} P_{(\beta)_i}}{k \cdot z} \tag{1}$$

where:

V_V – the volume fraction of the examined phase,

P_P – the fraction of points "hitting" the cross-sections of the examined phase β,

k – the number of grid applications,

$P_{(\beta)i}$ – the number of grid nodes incident on the cross-sections of the examined phase in the i-th grid application (i = 1, 2, ..., k),

z – the number of grid nodes.

The necessary number of grid applications for the assumed retained austenite volume fraction of 25% and the relative error of the analysis not exceeding 0.1 was calculated from Equation 2 and its value is 3.

$$k = \frac{u_\alpha^2 \cdot (1 - V_V)}{\gamma^2 \cdot z \cdot V_V} = 3 \tag{2}$$

where:

V_V – the volume fraction of retained austenite,

γ – the relative error of the analysis was assumed to be 0.1 along with the probability that the assessment error would not exceed the assumed value of 1 - α = 0.9 (α = 0,1). The value of u_α was read from the normal distribution tables (1.645),

z – the number of grid nodes.

The absolute error of the analysis was calculated from Equation 3.

$$\delta \leq u_\alpha \sqrt{\frac{P_p \cdot (1 - P_p)}{k \cdot z}} \tag{3}$$

Examinations were carried out using a TESCAN MIRA scanning electron microscope (Brno, Czech Republic), which is equipped with an EDS microanalyzer allowing for the analysis of the chemical composition of the alloy matrix and phases visible on metallographic sections. For the examined areas of martensite and retained austenite, a qualitative analysis was performed in the form of surface distribution of elements and a quantitative analysis in the form of chemical compositions in selected micro-areas, expressed in percent by weight. The surface distribution of elements such as Cr, Mn, Si, Ni and Mo and the respective quantitative analyses were performed for two areas of martensite and two areas of retained austenite, and in each of them three micro-areas were analyzed, calculating next the average chemical composition. The use of SEM with an FEG electron source, equipped with an EBDS detector provided by Symetry S2 (manufactured by Oxford Instruments, Abingdon, Great Britain), allowed for the acquisition of EBSD images of the occurring phases. The examinations were carried out on both etched samples (using a mixture of nitric acid and ethyl alcohol) and unetched samples.

3. Test results and discussion

Figure 8 shows characteristic microstructures at a magnification of 100x and 200x along with the areas where microcracks were formed due to the use of cooling media with different cooling intensities. In all cases, after heat treatment, the microstructure of the examined samples consisted of martensite and retained austenite. Cracks were observed in all tested samples

except the one cooled in air, and the appearing microcracks were running through the areas of both retained austenite and martensite. Yet, based on the examinations of the samples, it was not possible to clearly indicate the place of the initiation of microcracks and the privileged direction of their development. They occurred equally often in the areas of retained austenite and martensite. Figure 9 shows an example of the X-ray diffraction pattern of phases occurring in the tested samples. It confirms the presence of retained austenite, but based on this pattern it is difficult to accurately determine the volume fraction of the examined phase, and therefore the volume fraction V_v of retained austenite was calculated manually by the point method. Table 2 presents a relationship between the volume fraction of retained austenite and the type of heat treatment with the calculated absolute measurement error ±δ, while Table 3 compares the measured hardness values of both examined phases and their correlation with the heat treatment parameters. The results of all hardness measurements were presented, calculating next the average and the standard deviation ±δ. This presentation of the results illustrates their homogeneity and the phase structure of the microstructure.

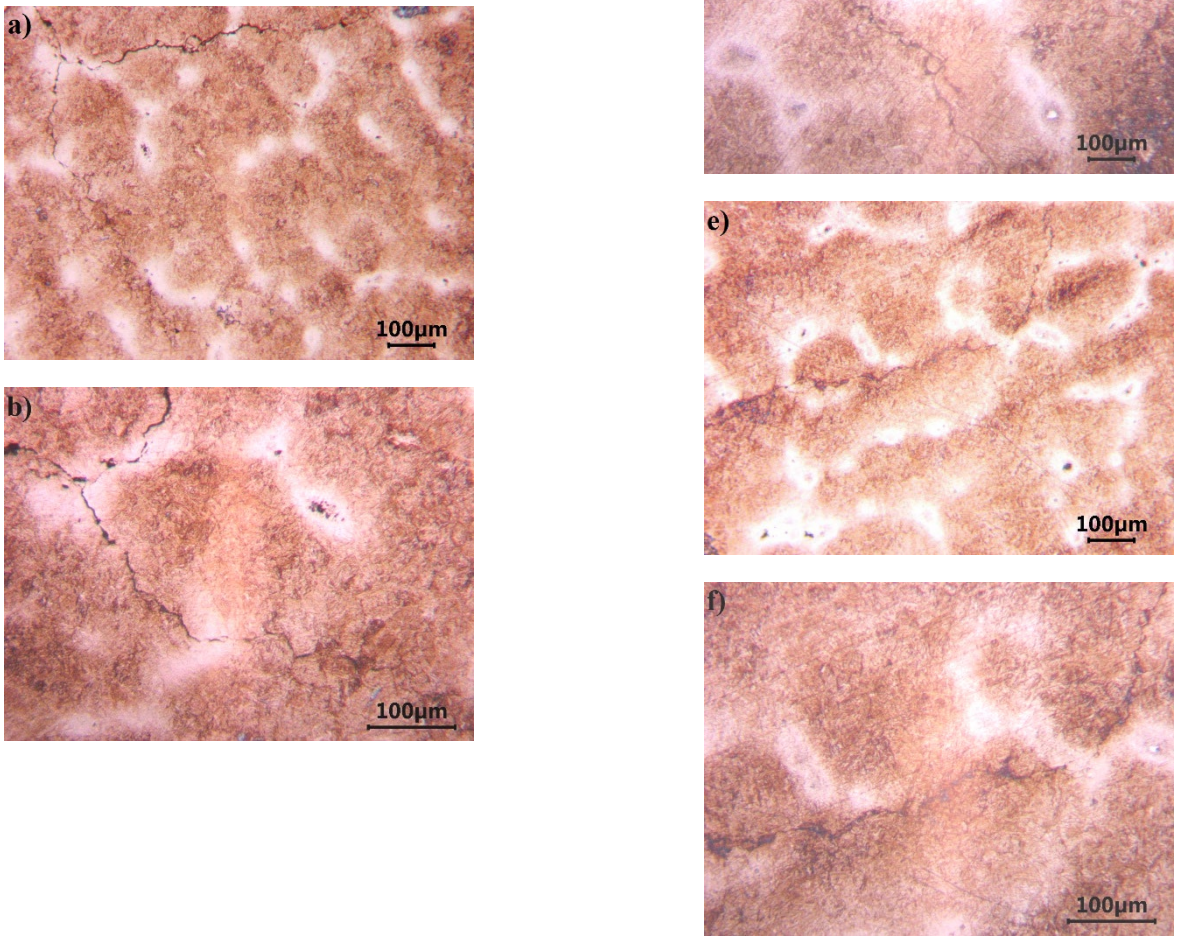

Fig. 8. Microstructure of the cast GX70CrMnSiNiMo2 steel after quenching: a, b) in water; c, d) in 10% HI; e, f) in 20% HI; dark martensite, light retained austenite; etched with nital

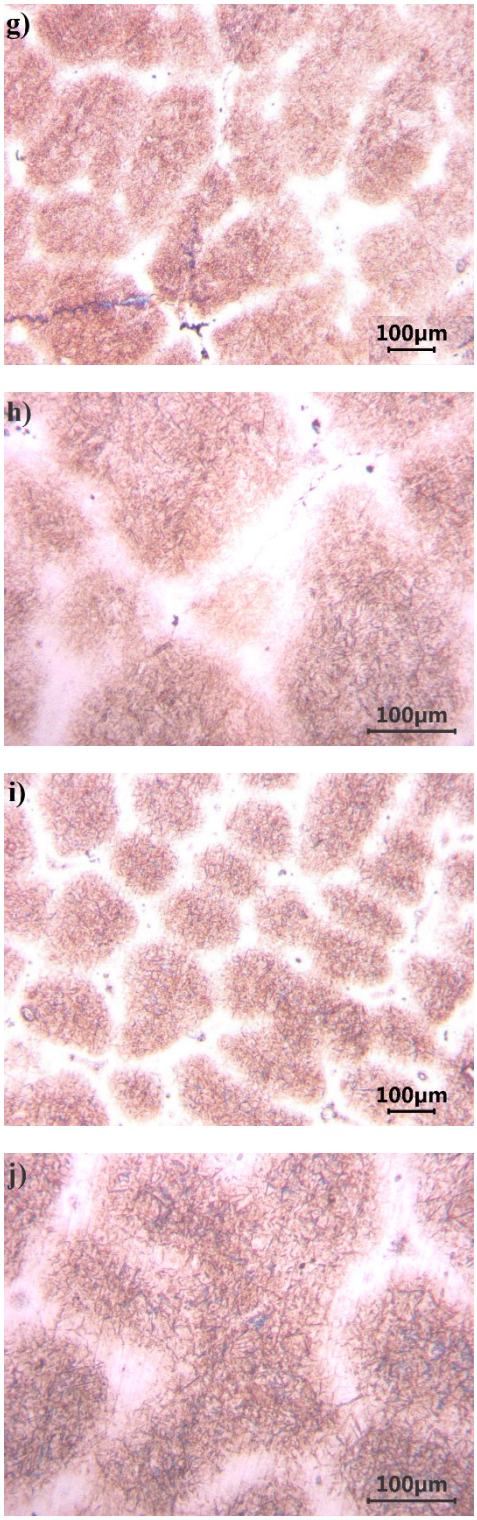

Fig. 8. Microstructure of the cast GX70CrMnSiNiMo2 steel after quenching: g, h) in 30% HI; and j) in air; dark martensite, light retained austenite; etched with nital

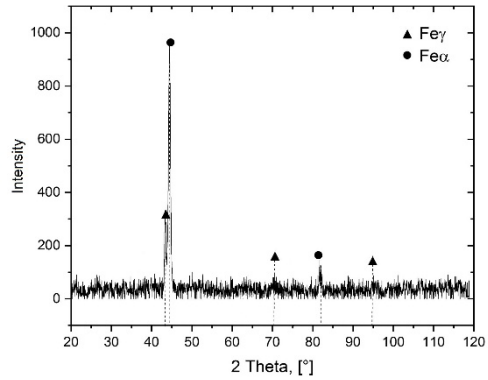

Fig. 9. Example of an X-ray diffractogram of samples after air quenching.

Table 2.
Heat treatment of the tested samples, volume fraction V_v of retained austenite

Heat treatment	V_v of austenite, % ±δ, %
930°C/0,7h/water	21.9 ±1.8
930°C/0,7h/ 10% HI	19.7 ±1.7
930°C/0,7h/ 20% HI	21.1 ±1.8
930°C/0,7h/ 30% HI	20.9 ±1.8
930°C/0,7h/air	31,1 ±2.0

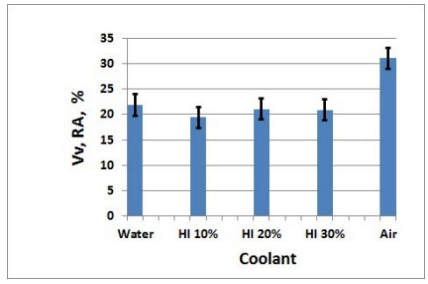

Fig. 10. Volume fraction of retained austenite vs type of cooling medium

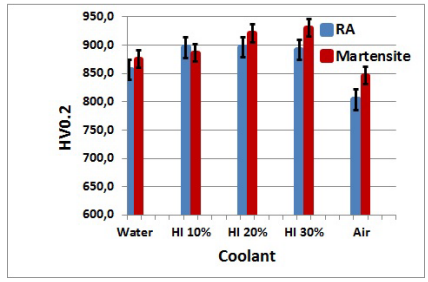

Fig. 11. Hardness of retained austenite and martensite vs type of cooling medium

Table 3.
Heat treatment of the tested samples, hardness of retained austenite and martensite

Heat treatment	Retained austenite		Martensite	
	HV0.2	Average HV0.2 ±δ		HV0.2
930°C/0.7h/water	821, 821, 882, 802, 841, 861, 861, 861, 927, 882	856 ±37	882, 841, 882, 882, 882, 861, 861, 975, 841, 841	875 ±40
930°C/0.7h/HI 10%	950, 975, 861, 861, 882, 882, 927, 950, 841, 821	895 ±52	975, 861, 861, 861, 882, 927, 882, 841, 841, 927	886 ±44
930°C/0.7h/HI 20%	882, 882, 950, 882, 904, 904, 904, 927, 904, 821	896 ±34	950, 927, 882, 882, 950, 950, 950, 950, 882, 882	921 ±34
930°C/0.7h/HI 30%	882, 882, 904, 927, 841, 904, 861, 927, 904, 882	891 ±27	904, 927, 975, 882, 882, 904, 975, 950, 975, 927	930 ±37
930°C/0.7h/air	732, 821, 749, 821, 802, 821, 821, 841, 821, 802	803 ±35	802, 802, 784, 861, 861, 821, 861, 882, 904, 882	846 ±41

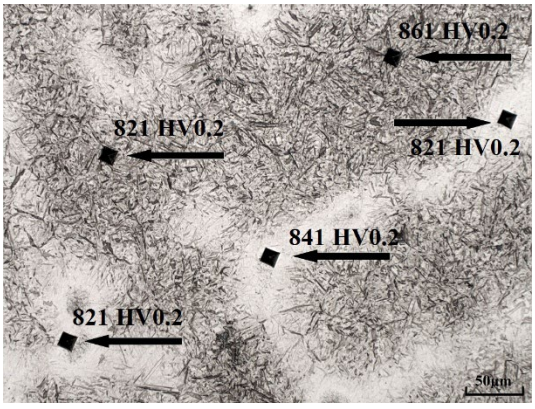

Fig. 12. Example of microstructures obtained in an air-quenched sample with visible imprints and hardness values in the areas of austenite and martensite

Figure 12 shows an example of microstructures with visible locations where the microhardness of both martensite and austenite was measured, wherefrom it can be concluded that the measured hardness values are similar.

The research has confirmed that, based on the calculated volume fraction of retained austenite and hardness of austenite and martensite in the tested samples related to the applied cooling intensity, it can be stated that the hardness of retained austenite is similar to that of martensite. The value can be as high as almost 900HV0.2 and shows a very weak dependence on the cooling intensity of the quenching medium. The effect of the type of cooling medium on the volume fraction of retained austenite, which amounts to about 21%, is also very weak. The exception is quenching in air, when the cooling rate is the lowest. Then the volume fraction V_v of retained austenite is the largest (31%) and its hardness is the lowest and decreases significantly to a value slightly above 800HV0.2, similarly to the hardness of martensite, which decreases on average to a value of almost 850 HV0.2.

The explanation for the occurring phenomena and changes in the V_v and HV parameters is be sought in the cooling rate of samples. Firstly, rapid cooling and accumulation of structural and thermal stresses increase the internal stresses so much that the consequence is cracking of the samples and high values of hardness. Secondly, cracking of the samples causes relaxation of internal stresses and further martensitic transformation, which results in a lower volume fraction of retained austenite. Thirdly, slow cooling in air significantly reduces the cooling rate during quenching and causes undercooling during transformation, which reduces both transformation rate and hardness. The cooling time is sufficiently long to induce not only a simultaneous relaxation of structural and thermal stresses, but also tempering of martensite at the stage of its formation. Therefore, for samples quenched in air, the largest volume fraction of retained austenite and the lowest hardness can be expected.

3.1. Segregation of alloying elements in the areas of retained austenite and martensite

Figure 13 shows examples of SEM images, where the surface distribution of elements such as C, Cr, Mn, Si, Ni, Mo was examined (Figs. 13b-13h), and the locations of analysis of the chemical composition of micro-areas are marked in the zone of both martensite and retained austenite (Fig. 13a). The analysis carried out did not show any visible differences in the content of the examined elements, chromium being the only exception (Fig. 13d). Only a few non-metallic inclusions rich in Mn and Mo were observed (Figs. 13e and 13g).

It was the quantitative analysis performed in two different fields of view for the examined elements in the individual areas of martensite and austenite (the measurement scheme and designation of points for both fields of view tested are marked in Figure 13a) that showed visible differences in the content of these elements. Based on the obtained results of the measured content of the examined chemical elements, presented in Tables 4 and 5, the following statements can be made.

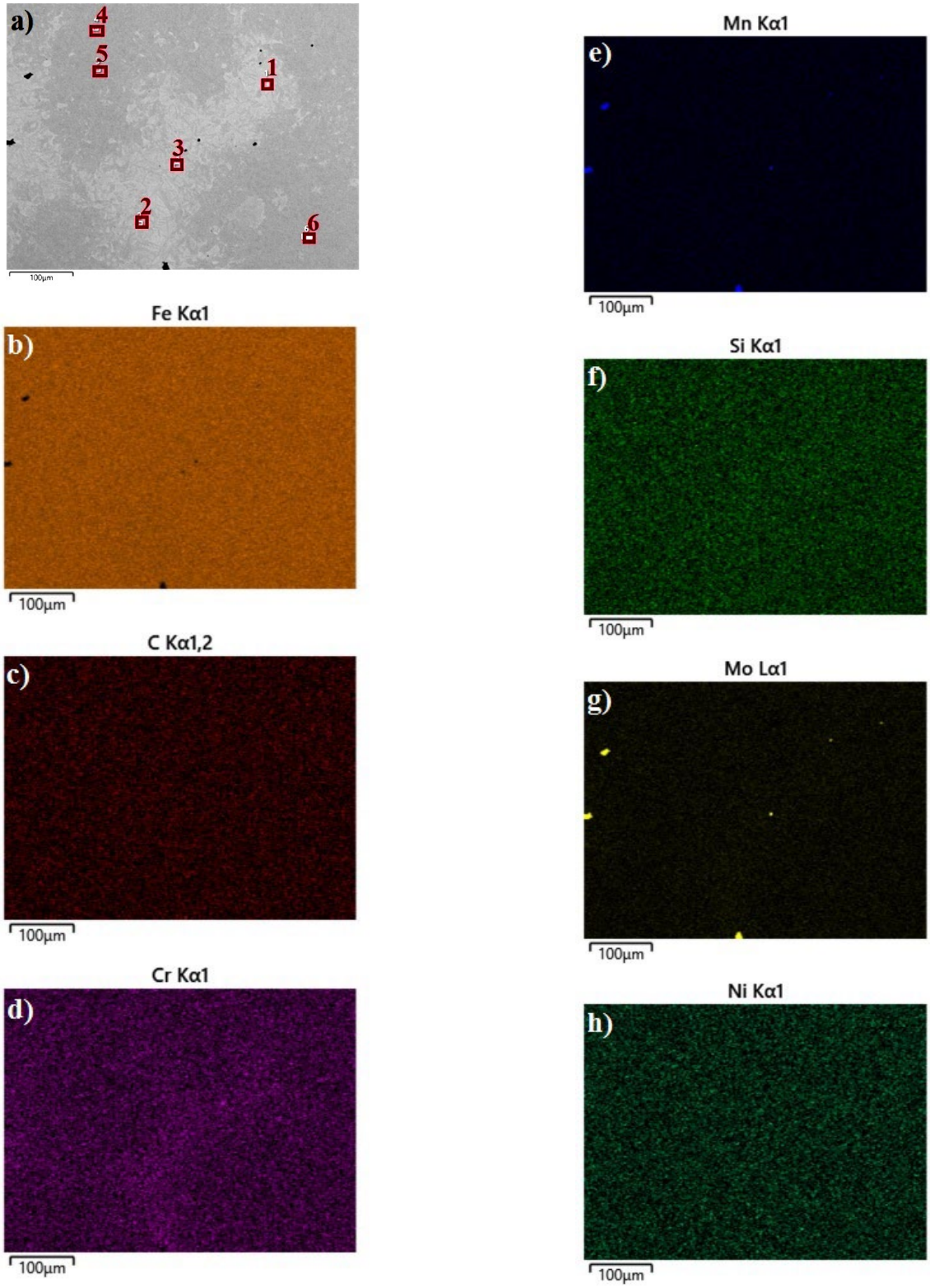

Fig. 13. Example of the surface distribution of elements such as Fe, C, Cr, Mn, Si, Ni, Mo in the area of retained austenite (points 1, 2 and 3) and martensite (points 4, 5 and 6)

Table 4.
Quantitative analysis in the areas of retained austenite (points 1, 2 and 3) and martensite (points 4, 5 and 6) according to the diagram in Figure 13a, first field of view

Location of analysis	[wt.%]						
	C	Si	Cr	Mn	Ni	Mo	Fe
point 1	5.2	0.5	1.2	1.0	0.7	0.6	Balance
point 2	4.7	0.6	1.3	0.9	0.7	0.6	Balance
point 3	5.1	0.6	1.5	0.8	0.7	0.8	Balance
Average	5.0	0.6	1.3	0.9	0.7	0.7	------
point 4	5.3	0.4	0.8	0.8	0.7	0.2	Balance
point 5	5.1	0.4	0.8	0.9	0.6	0.3	Balance
point 6	4.8	0.4	0.8	0.7	0.7	0.2	Balance
Average	5.1	0.4	0.8	0.8	0.7	0.2	------

Table 5.
Quantitative analysis in the areas of retained austenite (points 1, 2 and 3) and martensite (points 4, 5 and 6) according to the diagram in Figure 13a, second field of view

Location of analysis	[wt.%]						
	C	Si	Cr	Mn	Ni	Mo	Fe
point 1	5.1	0.6	2.0	0.8	0.9	1.5	Balance
point 2	5.0	0.6	1.3	0.9	0.7	0.7	Balance
point 3	5.2	0.5	1.7	1.0	0.7	1.0	Balance
Average	5.1	0.6	1.7	0.9	0.8	1.1	------
point 4	5.3	0.4	0.9	0.7	0.9	0.1	Balance
point 5	4.9	0.4	0.9	0.8	0.6	0.3	Balance
point 6	5.1	0.4	0.9	0.8	0.8	0.3	Balance
Average	5.1	0.4	0.9	0.8	0.8	0.2	------

The occurrence of retained austenite should be associated primarily with the high carbon content in the alloy, and with the primary segregation of elements such as Cr, Mo and, though to a lesser extent, Si and Mn, which most strongly lower the martensite finish temperature M_f. The greatest difference in the content of alloying elements in the area of retained austenite and martensite was observed for Cr, whose content (depending on the field of view) changed from 1.7-1.3 wt.% to 0.9-0.8 wt.%, and for Mo, whose content decreased from 1.1-0.7 wt.% in the area of retained austenite to 0.2 wt.% in the area of martensite. Si and Mn segregated to a much lesser extent, and their content in the area of retained austenite and martensite changed from 0.9 to 0.8 wt.% for Mn and from 0.6 to 0.4 wt.% for Si. No change in nickel content was observed; in the areas of both martensite and retained austenite it was similar and amounted to about 0.7-0.8 wt.%.

The high hardness of retained austenite was caused, firstly, by huge compressive stresses originating from martensite, and secondly, by alloy additives dissolved in austenite, which solution strengthened the retained austenite, and whose content in those areas was the highest. A combination of both these mechanisms makes the hardness of retained austenite close to the hardness of martensite and assuming values as high as 900HV0.2.

4. Conclusions

Based on the conducted studies of the chemical composition, microstructure, microhardness, microsegregation of alloying elements and volume fraction of retained austenite in the tested samples after different heat treatment variants, it can be concluded that:

1. Regardless of the medium used, the microstructure consists of martensite and retained austenite.
2. The emerging microcracks are running through the areas of both retained austenite and martensite.
3. It was not possible to indicate the place of the initiation of microcracks and the direction of their development.
4. The hardness of retained austenite is similar to that of martensite and is weakly dependent on the intensity of the cooling medium.
5. The type of cooling medium has but only an insignificant effect on the volume fraction of retained austenite.
6. Quenching in air raises the volume fraction of retained austenite to the highest level and reduces its hardness to the lowest level.
7. The greatest differences in the content of alloying elements in the areas of retained austenite and martensite were observed for Cr and Mo.
8. Si and Mn segregate to a much lesser extent.
9. Nickel content was observed to remain unchanged in both areas of martensite and retained austenite.
10. The high hardness of retained austenite is caused by structural stresses and solution strengthening.

Acknowledgements

Prepared from contract 16.16.170.654/B02

References

[1] Przybyłowicz, K. (1997). *Metal science.* Warszawa: WNT. (in Polish).

[2] Głownia, J. (2002). *Alloy steel castings-applications.* Kraków: Fotobit. (in Polish).

[3] Dobrzański, L. (2006). *Engineering materials and material design.* Warszawa: WNT. (in Polish).

[4] Metals Handbook. (1990). 10-th Ed., vol. 1. ASM International.

[5] Głownia, J., Tęcza, G., Sobula, S., Kalandyk, B., Dzieja, A. (2007). *Determination of the content and effect of residual austenite on the properties of cast L70H2GNM steel.* Research done for Metalodlew S.A., unpublished. (in Polish).

[6] Głownia, J. (2017). *Metallurgy and technology of steel castings.* Sharjah: Bentham Science Publishers.

[7] Stradomski, Z. (2010). *The role of microstructure in the wear behavior of abrasion-resistant cast steels.* Częstochowa: Wydawnictwo Politechniki Częstochowskiej. (in Polish).

[8] Wingens, T. (2021). Retained austenite benefits or avoidance requires dependable determination. In the 31st Heat Treating Society Conference and Exposition, 14-16 September 2021 (pp. 212-219). St. Louis, Missouri, USA. DOI: 10.31399/asm.cp.ht2021p0212.

[9] Kobasko, N.I., Aronov, M.A., Powell, J.A., Vanas J.H. (2009). Intensive quenching of steel parts: equipment and method. In the 7th IASME/WSEAS International Conference on Heat Transfer, Thermal Engineering and Environment (HTE '09), 20-22 August 2009 (pp. 153–158). Moscow, Russia. DOI: 10.13140/RG.2.2.17040.56328.

[10] Tęcza, G. (2023). Changes in the microstructure and abrasion resistance of tool cast steel after the formation of titanium carbides in the alloy matrix. *Archives of Foundry Engineering*. 23(4), 173-180. DOI: 10.24425/afe.2023.148961.

[11] Głownia, J., Tęcza, G., Sobula, S., Kalandyk, B. & Dzieja A. *Determination of the content and effect of residual austenite on the properties of cast L70H2GNM steel*. Research done for Metalodlew S.A., unpublished. (in Polish).

[12] Rothleutner, L. (2019, March 11). *Retained austenite significant for strength, toughness.* Retrieved September 15, 2024, from https://thermalprocessing.com/retained-austenite-significant-for-strength-toughness/.

[13] Xiong, X.C., Chen, B., Huang, M.X., Wang, J.F. & Wang, L. (2013). The effect of morphology on the stability of retained austenite in a quenched and partitioned steel. *Scripta Materialia*. 68(5), 321-324. DOI: 10.1016/j.scriptamat.2012.11.003.

[14] Sugimoto, K., Usui, N., Kobayashi, M. & Hashimoto, S. (1992). Effects of volume fraction and stability of retained austenite on ductility of TRIP-aided dual-phase steels. *ISIJ International.* 32(12), 1311-1318. DOI: 10.2355/isijinternational.32.1311.

[15] Tkachev, E., Borisov, S., Borisova, Y., Kniaziuk, T., Belyakov, A. & Kaibyshev, R. (2024). Austenite stabilization and precipitation of carbides during quenching and partitioning (Q&P) of low-alloyed Si–Mn steels with different carbon content. *Materials Science and Engineering A*. 895, 146212, 1-15. DOI: 146212. 10.1016/j.msea.2024.146212.

[16] Ma, T., Fu, B., Guan, W., Guo, Y., Fu, L. & Shan, A. (2024). Dissolution behavior of carbide in 4cr13 martensitic stainless steel during austenitizing. *Journal of Materials Engineering and Performance*. 34(6), 5394-5401. DOI: 10.1007/s11665-024-09509-0.

[17] Chen, X. & Li, Y.X. (2006). Investigation of the influence of austempering processing on retained austenite amount of austempered high silicon cast steel. 55, 284-287.

[18] Gu, J., Li, D., Liu, S. & Liu, Z. (2024). Microstructure and properties of Mn–Si–Cr alloy steel modified by quenching and partitioning. *Materials Testing.* 66(3), 305-315. DOI: 10.1515/mt-2023-0341.